Accepted Manuscript published as JME-26-0065. Accepted for publication: 20-Oct-2026
Check for updates

Temporal organization of leptin signaling reveals distinct regulatory roles for STAT3 and ETV6

Ekta Pathak[1,2,3], Miriam Bernecker[1,2,3,4], Noémi Mallet[1,2,3], Ann-Christin König[5], Ruth Gutierrez-Aguilar[1,2,6,7], Cristina Mencias[1,2,3,4], Sonja C. Schriever [1,2,3], Paul T. Pfluger [1,2,3,4,§]

Author affiliations:

[1] Research Unit NeuroBiology of Diabetes, Helmholtz Munich, 85764 Neuherberg, Germany

[2] Institute for Diabetes and Obesity, Helmholtz Munich, 85764 Neuherberg, Germany

[3] German Center for Diabetes Research, 85764 Neuherberg, Germany

[4] Division of Neurobiology of Diabetes, TUM School of Medicine and Health, Technical University of Munich, 81675 Munich, Germany

[5] Metabolomics and Proteomics Core, Helmholtz Munich, 85764 Neuherberg, Germany

[6] Unidad de Investigación en Obesidad, Facultad de Medicina, Universidad Nacional Autónoma de México (UNAM), 04510 Mexico City, Mexico

[7] Subdirección de Investigación Clínica, Dirección de Investigación, Instituto Nacional de Ciencias Médicas y Nutrición Salvador Zubirán (INCMNSZ), 14080 Mexico City, Mexico

[§] Correspondence to: Prof. Dr. Paul T. Pfluger

Research Unit NeuroBiology of Diabetes

Institute for Diabetes and Obesity

Helmholtz Munich

Ingolstaedter Landstr.1

Downloaded from journals.bioscientifica.com/jme/article-pdf/doi/10.1530/JME-26-0065/526775/jme-26-0065.pdf by [CU-1058505] | Helmholtz Zentrum Muenchen user on 27 October 2026

Copyright © 2026 the author(s)

D-85764 Neuherberg

Tel: 0049 89 3187 2104

paul.pfluger@helmholtz-munich.de

Short title: Temporal architecture of leptin signaling

Keywords: Leptin signaling dynamics, Etv6, Stat3, Transcription factor regulon activity, Pathway interactions

Word count: 4709

Abstract

Leptin regulates energy homeostasis through activation of its long-form receptor (*LepRb*), primarily via JAK2-dependent phosphorylation of STAT3. However, the temporal organization of leptin-induced transcriptional responses and how parallel signaling pathways contribute to these dynamics remain incompletely understood. Here, we established a *LepRb*-expressing hypothalamic cellular model to investigate the temporal architecture of leptin-induced transcription factors and pathways identified by transcriptome and proteome profiling at baseline (0 min), early (30 min), and late (180 min) time points. Overall changes in acute leptin stimulation were primarily reflected at the level of transcriptional and regulatory reprogramming. Proteomic remodeling mirrored the transcriptome but appeared smaller, likely due to assay insensitivity and slower dynamics of protein regulation, making the transcriptome the more informative kinetic readout. Structured transcriptional dynamics included the rapid activation of stress- and inflammatory-associated genes followed by sustained cytokine and interferon signaling modules. Transcription factor regulon and pathway activity inference identified coordinated activation of STAT, NF-κB, and MAPK-associated regulatory programs underlying these expression trajectories. CRISPR-Cas9-based deletion of *Stat3* markedly altered basal transcriptional states and attenuated leptin-induced gene expression while revealing activation of alternative signaling pathways. In contrast,

Downloaded from journals.bioscientifica.com/jme/article-pdf/doi/10.1530/JME-26-0065/526775/jme-26-0065.pdf by [CU-1058505] | Helmholtz Zentrum Muenchen user on 27 October 2026

Copyright © 2026 the author(s)

Accepted Manuscript published as JME-26-0065. Accepted for publication: 20-Oct-2026

Downloaded from journals.bioscientifica.com/jme/article-pdf/doi/10.1530/JME-26-0065/526775/jme-26-0065.pdf by [CU-1058505] | Helmholtz Zentrum Muenchen user on 27 October 2026

CRISPR-Cas9-based deletion of the ETS transcriptional repressor *Etv6* strongly affected baseline transcription but had minimal impact on leptin-induced regulatory dynamics. Together, these findings reveal a temporally organized regulatory architecture in which STAT3 governs stimulus-responsive transcriptional dynamics, whereas ETV6 primarily modulates baseline transcriptional states.

Introduction

Leptin is a key hormonal regulator of energy homeostasis that promotes a negative energy balance by suppressing food intake [1,2]. Its actions are mediated by the long form of the leptin receptor (LepRb), which activates intracellular signaling cascades, most prominently the JAK2-dependent STAT3 pathway [3,4]. STAT3-driven transcriptional programs are essential for maintaining energy homeostasis and body weight [5,6]. Although *LepRb* is expressed peripherally [7,8], its highest density is in the central nervous system, where leptin exerts its strongest metabolic effects [9,10].

Within the brain, *LepRb* is concentrated in hypothalamic circuits governing appetite control [11]. Agouti-related peptide (AgRP) neurons, which strongly express *LepRb*, are key drivers of feeding. Their activation during fasting or through chemo-/ optogenetic stimulation rapidly induces feeding [12], whereas leptin suppresses AgRP activity. Deletion of *LepRb* in AgRP neurons reduces leptin's anorexigenic effects and promotes hyperphagia and weight gain [13].

The heterogeneity of *LepRb*-expressing neurons complicates the in vivo dissection of leptin signaling, as transcriptional and signaling responses differ across cell types and brain regions [14]. In vitro systems have therefore been instrumental for defining core JAK-STAT, MAPK, and PI3K signaling pathways [15–17] and for dissecting post-translational events using modern proteomic platforms [18].

Copyright © 2026 the author(s)

Downloaded from journals.bioscientifica.com/jme/article-pdf/doi/10.1530/JME-26-0065/526775/jme-26-0065.pdf by [CU-1058505] | Helmholtz Zentrum Muenchen user on 27 October 2026

Emerging data further suggests that leptin's physiological effects unfold over distinct temporal scales. Real-time calcium imaging studies have shown that, unlike anorexigenic peptides such as PYY or CCK, which suppress AgRP neuron activity within minutes, leptin reduces AgRP neuronal activity more gradually over several hours [19]. Such delayed kinetics imply that leptin's sustained physiological effects are likely mediated not solely through rapid events such as protein phosphorylation, but also through longer-term mechanisms involving synaptic modulation, circuit remodeling and likely, transcriptional reprogramming. Downstream leptin effectors, including STAT3, STAT5, SOCS3, and PTP1B [20–22] are well-positioned to mediate such gene expression changes and feedback control.

While STAT3 phosphorylation is considered the dominant transcriptional effector of LepRb, additional pathways, including other STAT proteins, MAPK, PI3K-AKT, and NF-κB, also contribute to leptin-induced gene regulation [23,24]. How these pathways integrate to shape temporally ordered transcriptional dynamics remains poorly understood.

Beyond the direct activation of STAT proteins, transcriptional regulators downstream of *LepRb* signaling may further shape baseline transcriptional states and feedback regulation. ETS-family transcription factors have emerged as additional regulators of leptin signaling. ETV5 contributes to leptin-induced activation of POMC neurons and energy balance [25,26], while ETV6 represses STAT3 target genes [27] and is regulated in leptin-responsive neurons [28–31]. However, whether ETV6 influences acute leptin-induced transcriptional responses is unknown.

To address these questions, we used a hypothalamic neuronal cell line engineered to overexpress *LepRb*, enabling high-resolution temporal mapping of leptin-induced signaling, transcriptional regulation, and feedback architecture. We performed

Copyright © 2026 the author(s)

Accepted Manuscript published as JME-26-0065. Accepted for publication: 20-Oct-2026

Downloaded from journals.bioscientifica.com/jme/article-pdf/doi/10.1530/JME-26-0065/526775/jme-26-0065.pdf by [CU-1058505] | Helmholtz Zentrum Muenchen user on 27 October 2026

transcriptomic profiling at baseline, 30 min, and 180 min after leptin stimulation, integrated these data with transcription factor and pathway activity inference, and complemented them with proteomic profiling at baseline and 180 min. Lastly, using *Stat3*- and *Etv6*-deleted cell models, we examined how loss of these factors alters basal and leptin-induced gene regulatory programs, with particular attention to regulatory interaction effects reflecting compensatory or rewired signaling.

Methods

Cell Culture

CLU177 cells were cultured in 6-well plates with high glucose DMEM (Invitrogen, #41965039), with 10% heat-inactivated FBS and 1% Pen/Strep. Transfection of the pCAG-2A-H2B Venus_mOBRb-HA plasmid, that facilitates cytosolic expression of the long isoform of the leptin receptor in parallel with a nuclear GFP signal, was carried out using the FuGene® HD transfection reagent (Promega, Madison, WI, USA). 24h post transfection, cells were stably selected with 3 µg/ml puromycin. Based on the GFP signal CLU177mOBRb cells with high LepR expression were isolated by FACS and cultured in full medium containing puromycin. For leptin stimulation assays, cells were placed in starvation medium (DMEM, with 1% FBS) 2 h prior to leptin stimulation. Recombinant murine leptin was added to the cells at given concentrations (10 pM – 100 nM). Cells were stimulated for the indicated times with leptin, washed twice with ice-cold PBS and then snap frozen at -80°C. For immunofluorescence detections of HA-tagged LepR and pSTAT3, cells were grown on glass coverslips, treated and fixed using 4% PFA. For proteome analyses, cells were directly scraped in sodium deoxycholate buffer (4% SDC

Copyright © 2026 the author(s)

Downloaded from journals.bioscientifica.com/jme/article-pdf/doi/10.1530/JME-26-0065/526775/jme-26-0065.pdf by [CU-1058505] | Helmholtz Zentrum Muenchen user on 27 October 2026

and 100 mM Tris pH8.5) and subjected to protein digestion following a modified filter-aided sample preparation (FASP) protocol as described previously [32,33]. Detailed procedures for protein and RNA extraction, Western Blotting, quantitative PCR, immunofluorescence detection and FASP digestion can be found in the Supplemental Material.

Stat3 and Etv6 deleted CLU177mOBRb cell lines

Genomic deletions were induced using a CRISPR–Cas9–based dual‐guide strategy. In brief, two single-guide RNAs (sgRNAs) were designed to flank the genomic region of interest (Suppl. Table 1) using the CRISPOR software (https://crispor.gi.ucsc.edu/). For delivery of the editing components, CLU177mOBRb cells were electroporated with the pX330-U6-Chimeric_BB-CBh-hSpCas9 expression constructs (Addgene plasmid #42230) [34], encoding Cas9 and the paired sgRNAs. After blasticidin selection (10 µg/ml for 48h), single clones were picked from the mixed cell population and expanded. Genomic DNA was isolated with the Wizard® Genomic DNA Purification Kit (Promega, #A1120, Madison, WI, USA) and subjected to PCR amplification with specific primers (Suppl. Table 2) and Sanger sequencing to corroborate the successful deletion.

RNA sequencing

RNA integrity of the total RNA extracted from CLU177mOBRb WT and DEL cell lines was assessed using the Agilent 2100 Bioanalyzer, and samples with an RNA Integrity Number (RIN) ≥ 7 were used for library preparation. RNA concentration was measured with a Qubit fluorometer (Thermo Fisher Scientific). Libraries for biological replicates per condition (n=8 for WT cells and n=4 for Stat3Δ or Etv6Δ clones) were generated using the Illumina Stranded mRNA Ligation kit at the Core facility (CF-GEN) at Helmholtz Munich, following

Copyright © 2026 the author(s)

 Accepted Manuscript published as JME-26-0065. Accepted for publication: 20-Oct-2026

Downloaded from journals.bioscientifica.com/jme/article-pdf/doi/10.1530/JME-26-0065/526775/jme-26-0065.pdf by [CU-1058505] | Helmholtz Zentrum Muenchen user on 27 October 2026

the kit's instructions. After a final quality control (QC), equimolar amounts of indexed libraries were pooled and sequenced on an Illumina NovaSeqX+ platform (Illumina, San Diego, CA, USA). Sequencing was performed with a paired-end 2 × 100 bp configuration aiming for 30 million reads per sample. Base calling and demultiplexing were performed using Illumina's bcl2fastq software.

LC-MS/MS measurements

Liquid chromatography-mass spectrometry (LC-MS/MS) analysis was performed in data-dependent acquisition (DDA) mode on a Q-Exactive HF-X mass spectrometer (Thermo Scientific) coupled to a nano-RSLC (Ultimate 3000 RSLC; Dionex). Tryptic peptides were loaded on a C18 trap column (300 µm × 5 mm, Acclaim PepMap100 C18, 5 µm, 100 Å, LC Packings) at 30 µl/min flow rate and separated on a C18 analytical column (nanoEase MZ HSS T3 Column, 100 Å, 1.8 µm, 75 µm × 250 mm, Waters) using a 95-min nonlinear gradient from 3 - 40% acetonitrile in 0.1% formic acid at 250 nl/min. Full MS scans were acquired at 60,000 resolution (300-1500 m/z; AGC 3x 10^6; 30 ms). The top 15 doubly charged or higher precursor ions were selected for MS/MS (15,000 resolution; AGC 5x 10^2; 50 ms; NCE28; 30 s dynamic exclusion). Spectra were recorded in profile mode. Detailed procedures on protein identification and label-free quantification are given in the Supplemental Material.

Bioinformatical and statistical analyses

Statistical analyses for Western Blotting and qPCR results were conducted using GraphPad Prism (V. 11), with significance set at $P \leq 0.05$ under the assumption of normality. Groups were compared using One-Way ANOVA with Dunnett's post-hoc tests. Bioinformatic methods related to alignment, quantification, and transcriptomic and

Copyright © 2026 the author(s)

Downloaded from journals.bioscientifica.com/jme/article-pdf/doi/10.1530/JME-26-0065/526775/jme-26-0065.pdf by [CU-1058505] | Helmholtz Zentrum Muenchen user on 27 October 2026

proteomic data analyses, including the respective statistical assessments, were conducted using R, as described in the respective sections provided with the Supplemental Material.

Results

Generation of leptin receptor overexpressing hypothalamic cells

The cell line CLU177, generated from adult murine hypothalami, features mature neuron-like transcriptional signatures of hypothalamic developmental lineages residing within the arcuate nucleus [35] (Suppl. Fig. 1A,B), but expresses low endogenous *LepRb* and is largely unresponsive to leptin (Suppl. Fig. 1C). To enable detailed analysis of leptin signaling, we generated a stable line overexpressing HA-tagged murine *LepRb* (mOBRb) together with a Venus reporter (Fig. 1A). Leptin exposure for 20 min induced robust STAT3 and ERK phosphorylation, peaking at 1–10 nM (Fig.1B,C; Suppl. Fig. 1D-F). Immunofluorescence confirmed strong P-STAT3 induction after 20 min of 10 nM leptin relative to untreated cells (Fig. 1D). Using 10 nM leptin, qPCR showed that 30- and 180-min stimulation reliably activated early (*Atf3*, *Socs3*, *JunB*) and late (*Steap4*) transcriptional markers (Fig. 1E; Suppl. Fig. 1G).

Having established these conditions, we profiled the transcriptome at 0, 30, and 180 min, and the proteome at 0 and 180 min (Fig. 1F). Principal Component Analyses (PCA) revealed clear temporal separation in transcriptomes (Fig. 1G), while proteomic separation was less pronounced (Fig. 1H). Leptin induced large transcriptional changes: without a fold change (FC) cutoff, 746 differentially expressed genes (DEGs) at 30 min and 5,503 DEGs at 180 min ($p_{adj} < 0.05$; Suppl. File SF1), with ± 1 FC cutoff 169 DEGs up and 9

Copyright © 2026 the author(s)

 Accepted Manuscript published as JME-26-0065. Accepted for publication: 20-Oct-2026

Downloaded from journals.bioscientifica.com/jme/article-pdf/doi/10.1530/JME-26-0065/526775/jme-26-0065.pdf by [CU-1058505] | Helmholtz Zentrum Muenchen user on 27 October 2026

DEGs down at 30 min, and 424 DEGs up and 273 DEGs down at 180min (Fig. 1I). In contrast, proteomics identified only 24 up- and 3 downregulated differentially abundant proteins (DAPs) between 0 and 180 min (p_{adj} < 0.05; ± 1 FC cutoff; Fig. 1I; Suppl. Fig. 1H,I; Suppl. File SF1). Transcriptome–proteome correlation was low (Fig. 1J), indicating that proteomic depth and the chosen time point of 180 min in our assays may have contributed to an incomplete capture of leptin-induced responses at the protein level. Consequently, downstream analyses focused primarily on transcriptomic datasets to dissect leptin-regulated signaling networks in CLU177mOBRb cells.

Distinct leptin-induced gene expression trajectories in CLU177mOBRb (WT) cells

The analysis of DEGs after 30 or 180 min of leptin stimulation revealed pronounced temporal shifts in gene regulation (Fig. 2A,B), and K-means clustering (k=5) of pooled DEGs across all time points identified distinct expression trajectories (Fig. 2C). Distinct cluster centroids were next calculated by averaging expression values across all genes within each k-means cluster at each time point (0, 30, and 180 min) and defined as: EarlyUp (C3), UpThenDown (C2), LateUp (C4), LateDown (C1), and Mixed/Other genes (C5) (Fig. 2D). Representative genes exhibiting these patterns are shown in Suppl. Fig. 2A-C.

Functional enrichment of the major upregulated clusters (C2, C3, C4) revealed a structured, time-dependent inflammatory program (Fig. 2E; Suppl. File SF1). Early clusters C2 and C3 showed strong enrichment of TNFα/NF-kB signaling, consistent with rapid early inflammatory activation [36,37]. C2 and C3 additionally displayed Hypoxia and p53 pathway signatures, indicating a stress-linked early response. C3 exhibited a broader intermediate inflammatory profile, enriched for IFN-γ Response, IL-2/STAT5, IL-

Copyright © 2026 the author(s)

Downloaded from journals.bioscientifica.com/jme/article-pdf/doi/10.1530/JME-26-0065/526775/jme-26-0065.pdf by [CU-1058505] | Helmholtz Zentrum Muenchen user on 27 October 2026

6/JAK/STAT3, Complement, Apoptosis, and TGF-β. The late-induced cluster C4 retained these inflammatory modules and gained IFN-α Response and EMT signatures, reflecting sustained pathway engagement at 180 min [38]. Clusters 1 and 5 showed no significant enrichment.

Next, we tested whether the transcriptional response observed in hypothalamic CLU177 cells recapitulates leptin action in vivo. Heyward et al. [29] had identified the translatome of AgRP neurons from mice treated with vehicle or 5 mg/kg leptin (180 min) after an overnight fast. We projected the 128 differentially expressed, leptin-induced genes identified by Heyward to our CLU177 WT leptin time course, and resolved these genes by K-means clustering into four distinct temporal expression modules (Fig. 2F). The largest cluster (cluster 1; n = 52) comprised genes with maximal expression at 180min, reminiscent of our LateUp centroid profile. Notably, 92% of these genes were significantly upregulated in the Heyward data, i.e. 180 min after leptin injections in mice (Suppl. Fig. 2D). Heyward genes of cluster 2, which were mostly upregulated in AgRP neurons of mice, peaked at 30 min in our cell data, reminiscent of the two EarlyUp and UpThenDown centroid profiles. Heyward genes of cluster 3, which showed a mix of up- and downregulation in vivo, were downregulated at 180 min in our data, consistent with the LateDown centroid profile. A 4th cluster, largely upregulated in the Heyward data, did not show any up- or downregulation in our cells (Suppl. Fig. 2E), hinting at an AgRP neuron-specific gene control that is not fully captured in our cell culture model. Nonetheless, ourr comparison to the mouse data indicates that the CLU177mOBRb cell line captures key temporal features of the in vivo transcriptional response to leptin.

Copyright © 2026 the author(s)

 Accepted Manuscript published as JME-26-0065. Accepted for publication: 20-Oct-2026

Downloaded from journals.bioscientifica.com/jme/article-pdf/doi/10.1530/JME-26-0065/526775/jme-26-0065.pdf by [CU-1058505] | Helmholtz Zentrum Muenchen user on 27 October 2026

Regulon-based transcription-factor and pathway activity dynamics during leptin stimulation in WT cells

To resolve regulatory dynamics downstream of leptin, we inferred transcription-factor (TF) and pathway (PW) activities from transcriptomes using DoRothEA [39] and PROGENy [40] (Fig. 3A). DoRothEA estimates TF activity from curated signed TF–target regulons, whereas PROGENy infers pathway activity from perturbation-derived transcriptional footprints, capturing downstream consequences rather than expression of canonical pathway components.

K-means clustering (k=4) of TF activity scores revealed four temporal regulon modules (Fig. 3B). EarlyUp (module 3) showed strong 30min activation of STAT1/3/5A, NFKB1, JUN, ETV4, ESR1, CEBPB, TBP, and ELF1 regulons (Fig. 3C). UpThenDown (module 2) displayed transient early activation of e.g. HIF1A, SP1 or JUNB returning to baseline by 180 min (Fig. 3D). LateUp (module 4), including MYC, FOXK2, CREB3 and BATF, rose progressively and peaked at 180 min (Fig. 3E). LateDown (module 1) showed reduced activity at 180 min, including STAT4, KLF3, GABPA, and MEF2A (Fig. 3F). These TF modules aligned with the gene expression trajectories in Fig. 2C: EarlyUp TFs matched EarlyUp genes (cluster 3), UpThenDown TFs aligned with clusters 2–3, LateUp TFs matched LateUp genes (cluster 4), and LateDown TFs correlated with LateDown and UpThenDown genes (clusters 1–2) (Fig. 3G).

PROGENy pathway analysis (Suppl. Fig. 3A) showed rapid activation of pro-inflammatory and stress-associated TNFα, NF⍰kB, and MAPK signaling at 30 min that persisted at lower levels at 180 min, whereas JAK–STAT and VEGF increased more gradually. Quantification revealed the highest activity for TGF⍰β, followed by MAPK, VEGF, and TNFα at all time points (Suppl. Fig. 3B). Correlation analysis linked EarlyUp genes (cluster 3) most

Copyright © 2026 the author(s)

Downloaded from journals.bioscientifica.com/jme/article-pdf/doi/10.1530/JME-26-0065/526775/jme-26-0065.pdf by [CU-1058505] | Helmholtz Zentrum Muenchen user on 27 October 2026

strongly with TNFα, NF‑kB, TGF‑β, MAPK, and JAK–STAT; UpThenDown genes (cluster 2) with TGF‑β, Hypoxia, and WNT; and LateDown and LateUp genes (clusters 1 & 4) with VEGF and JAK–STAT pathway activities (Suppl. Fig. 3C).

Given the central role of JAK–STAT signaling in leptin action, with STAT3 serving as one of its principal transcriptional effectors, we next examined the temporal regulation of canonical STAT3 target genes. This analysis was motivated by the observation that JAK–STAT pathway activity increased progressively over time and that STAT family members were represented across all transcriptional response modules. Consistent with the heterogeneous dynamics observed at the pathway and gene-module level, canonical STAT3 target genes displayed diverse temporal expression profiles following leptin stimulation, with most targets induced at 30 min (e.g. Socs3) and subsets maintaining either elevated (e.g. Etv6) or reduced (e.g. Bcl2) expression at 180 min (Fig. 3H).

Together, these results are consistent with leptin acting as adipocytokine that induces coordinated and time-resolved TF activities and pathways such as KLF6, NF-kB, TNFα, MAPK or JAK-STAT(3) which are reminiscent for a broad pro-inflammatory, catabolic and stress-related cell state.

Stat3 deletion alters basal and leptin-induced transcriptional dynamics

To characterize how loss of this key leptin effector reshapes the leptin‑responsive regulatory landscape, and to establish a basis for dissecting downstream pathway crosstalk, we generated *Stat3*‑deleted (Stat3Δ) CLU177mOBRb single cell clones using CRISPR‑Cas9 (Fig. 4A) and confirmed the complete loss of STAT3 protein expression (Suppl. Fig. 4A-C). Leptin exposure of clone Stat3Δ1, henceforth named

Copyright © 2026 the author(s)

 Accepted Manuscript published as JME-26-0065. Accepted for publication: 20-Oct-2026

Downloaded from journals.bioscientifica.com/jme/article-pdf/doi/10.1530/JME-26-0065/526775/jme-26-0065.pdf by [CU-1058505] | Helmholtz Zentrum Muenchen user on 27 October 2026

Stat3Δ, corroborated Stat3 mRNA deficiency (Fig. 4B) and revealed substantial baseline rewiring in a transcriptome analysis, with 648 upregulated and 1,423 downregulated genes in Stat3Δ vs WT cells (Fig. 4C,D; Suppl. File SF2). qPCR-based analyses of additional clones Stat3Δ 2 and 3 demonstrated that similar expression changes of key target genes in all three clones are likely biologically significant and not an artefact of the clonal expansion or CRISPR off-target effects (Suppl. Fig. 4D-K). Enrichment analysis indicated increased activity of receptor tyrosine kinase (RTK), MAPK, ERK and PI3K/PKB and in general phosphorylation‐associated pathways, suggesting broad compensatory signaling (Fig. 4E). Baseline TF activities were decreased for STAT3, STAT5B, FOS, RELA, NF‐κB1 and CEBPB, whereas STAT5A and EGR1 were elevated (Fig. 4F). Correspondingly, JAK–STAT and TGF‐β pathway activities were reduced (Fig. 4G), and STAT3‐target scores, calculated from average expression levels of high-confidence STAT3-activated target genes and z-scored across samples, were strongly diminished (Fig. 4H; heatmap: Suppl. Fig. 5; Suppl. File SF3)

Leptin stimulation further highlighted the dominant effect of genotype. PCA showed a clear separation between WT and Stat3Δ along PC1, with leptin‐induced variation captured on PC2 (Fig. 4I). Across time points, we identified 400 commonly upregulated and 859 commonly downregulated genes between genotypes, indicating dominant genotype-dependent transcriptional differences, whereas comparatively fewer DEGs exhibited leptin- or time‐specific regulation (Fig. 4J; Suppl. Fig. 6A,B).

Proteomic profiling recapitulated the transcriptomic regulation in direction and magnitude (0 min: Fig. 4K; 180 min: Suppl. Fig. 6C; Suppl. File SF2). Accordingly, transcript–protein correlations were positive at both time points (Fig. 4L; Suppl. Fig. 6D),

Copyright © 2026 the author(s)

Downloaded from journals.bioscientifica.com/jme/article-pdf/doi/10.1530/JME-26-0065/526775/jme-26-0065.pdf by [CU-1058505] | Helmholtz Zentrum Muenchen user on 27 October 2026

with 450 up-/ 350 down-concordant pairs at baseline and 456 pairs up/ 209 down at 180 min (Suppl. Fig. 6E,F).

STAT3 is required for coordinated leptin-induced TF and PW interactions

To assess how STAT3 loss alters the leptin-evoked transcriptional architecture, we compared early- and late-response gene sets between WT and Stat3Δ cells. Both EarlyUp (cluster 3) and LateUp (cluster 4) signatures were blunted in Stat3Δ cells (Fig. 5A, heatmaps: Suppl. Fig. 7A,B). We next examined genotype-by-leptin interaction effects (Stat3Δ:Leptin) on TF and PW activities, focusing on regulons and pathways significantly affected at any time point (see earlier Figs. 3B and 3C). This revealed broad perturbations across TF modules (Fig. 5B). STAT3 and STAT5A/B showed persistently reduced activity, whereas STAT1, STAT4, and STAT6 displayed increased interaction effects at 180 min, paralleling elevated JAK–STAT PW activity (Fig. 5C). Target-score analyses confirmed consistently reduced STAT3-target expression (Fig. 5D) and markedly increased STAT1-target activation at 180 min (Fig. 5E).

MAPK-linked regulons showed a similar pattern: reduced TF activity interactions at 30 min, followed by strong increases at 180 min for JUN, JUNB, ETS1, ELK4, RARA, CREB1, EGR1 (Fig. 5B), coinciding with elevated MAPK target scores (Fig. 5F). CREB1 and KLF6, both MAPK/JAK-STAT–responsive transcriptional integrators [41], showed pronounced late-phase activation in Stat3Δ cells (Fig. 5G,H). NF-κB family members demonstrated reduced interaction effects at 30 min but partial recovery by 180 min, reflected in the time-dependent normalization of NF-κB and TNFα PW activity and target scores (Fig. 5B,C,I). Additional TF target scores displayed genotype-specific temporal rewiring, including STAT4/6, ETS1, FOXK2, JUN, and JUNB (Suppl. Fig. 8A). Broader screening of all

Copyright © 2026 the author(s)

 Accepted Manuscript published as JME-26-0065. Accepted for publication: 20-Oct-2026

Downloaded from journals.bioscientifica.com/jme/article-pdf/doi/10.1530/JME-26-0065/526775/jme-26-0065.pdf by [CU-1058505] | Helmholtz Zentrum Muenchen user on 27 October 2026

regulons revealed further perturbation, for instance, interferon-associated (IRF1/2/3/9) TF or EGFR PW activities (Suppl. Fig. 8B).

At the gene level, Stat3Δ:Leptin interaction analysis identified 4 up- / 42 down-regulated genes at 30 min and 319 up- /198 down-regulated genes at 180 min (Fig. 5J; Suppl. File SF4). Several genes switched in regulatory direction depending on genotype and time (Fig. 5K), forming distinct expression modules (Fig. 5L). Integration with proteomics confirmed Stat3Δ□specific, leptin□responsive DAPs (Fig. 5M; Suppl. Fig. 8C,D; Suppl. File SF4).

Together, these findings show that leptin signaling includes a multi-layered regulatory network of TFs and pathways in which STAT3 acts as a central regulatory hub. Although Stat3 deletion triggered extensive activation of alternative transcription factors and pathways, these changes did not restore the canonical leptin-induced transcriptional program, indicating transcriptional network rewiring rather than functional replacement of STAT3.

Etv6 deletion causes major basal transcriptional changes

Prompted by recent reports implicating ETV5 in leptin-induced activation of POMC neurons [25,26], we next examined a potential role for the ETS family member ETV6. ETV6 is a transcriptional repressor [42] and has been shown to function as a suppressor of STAT3 activity [27]. Given recent evidence demonstrating leptin-induced *Etv6* expression in mouse AgRP neurons [28–31], which we corroborated in our data (Fig. 2F), we generated two single Etv6Δ cell clones, with targeting confirmed by sequencing and qPCR (Suppl. Fig. 9A,B). Clone 1, from hereon named Etv6Δ, was then stimulated with leptin for 30 or 180 min

Copyright © 2026 the author(s)

Downloaded from journals.bioscientifica.com/jme/article-pdf/doi/10.1530/JME-26-0065/526775/jme-26-0065.pdf by [CU-1058505] | Helmholtz Zentrum Muenchen user on 27 October 2026

(Fig. 6A). *Etv6* mRNA was absent in Etv6Δ cells, confirming the deletion, whereas *Etv6* expression in WT cells was induced by leptin (Fig. 6B). Known ETV6 target genes [43], i.e. *Ptprc*, *Itgb2*, *Kcnj2*, *Cerkl*, *Fgf2*, *Rasgap1*, *Osr2* and *Sptbn2*, were upregulated in Etv6Δ cells, consistent with loss of repression (Fig. 6C). Although *Stat3* expression was unchanged (Fig. 6D), STAT3-target scores were strongly elevated at baseline in Etv6Δ cells (Fig. 6E), aligning with ETV6 being positioned downstream of STAT3, acting as a negative regulator of STAT3 activity but not expression.

PCA showed a marked baseline separation between WT and Etv6Δ cells (PC1), which persisted after leptin stimulation, while PC2 captured the leptin-dependent variance (Fig. 6F). At baseline, Etv6Δ cells displayed 574 upregulated and 806 downregulated DEGs (Fig. 6G; Suppl. File SF5). Upregulated genes at baseline were enriched for pathways linked to dendritic spine morphogenesis, Wnt signaling, and mitochondrial calcium import, whereas downregulated genes involved superoxide generation, negative regulation of cytokine/growth factor signaling, and axonogenesis (Fig. 6H; Suppl. File SF5). Comparing common DEGs across time points, we found a profound overlap of 356 and 542 up- and down-regulated DEGs at 0, 30 and 180min (Fig. 6I; Suppl. Fig. 9C,D). These findings indicate that Etv6 deletion primarily establishes a persistent genotype-dependent transcriptional state that is maintained throughout the leptin time course. Top up- and downregulated genes commonly deregulated at all time points were visualized in a heatmap and functionally categorized (Fig. 6J). Selected genes were moreover assessed by qPCR in both Etv6Δ clones, revealing similar expression dynamics and thus a likely absence of clonal expansion artifacts or CRISPR-off-target effects (Suppl.Fig. 9E-J). Although fewer, DEGs exclusively up- or downregulated at 30 or 180 min indicated that

Copyright © 2026 the author(s)

 Accepted Manuscript published as JME-26-0065. Accepted for publication: 20-Oct-2026

Downloaded from journals.bioscientifica.com/jme/article-pdf/doi/10.1530/JME-26-0065/526775/jme-26-0065.pdf by [CU-1058505] | Helmholtz Zentrum Muenchen user on 27 October 2026

Etv6 also contributes to leptin-induced transcriptional responses, which we examined next.

Modest effects of *Etv6* deletion on leptin-induced transcriptional and regulatory responses.

Comparison of WT and Etv6Δ cells showed that EarlyUp (cluster 3) and LateUp (cluster 4) induction patterns were largely preserved after leptin stimulation (Fig. 7A; heatmaps: Suppl. Fig. 10A,B). In the TF and pathway activity interaction analysis (Etv6Δ:Leptin), no regulons or pathways reached significance after multiple-testing correction. We nonetheless visualized all the major TF and all pathway activities that were significant in our WT comparison of Figs. 3B and 3H and found, although of lower magnitude and non-significant, directional changes in the activities of MAPK, NF-κB, and TNFα signaling (Fig. 7B).

Differential expression analysis (FDR < 0.05; $|\log_2 FC| \geq 0.5$) nonetheless identified a small set of Etv6Δ-specific leptin-responsive genes, particularly between 30 and 180 min (Fig. 7C,D; Suppl. File SF6). Examples such as *Nox4*, *Sfmbt2*, *Fam13a*, and *Peg10* illustrate these minor, late-phase, genotype-specific changes (Fig. 7E). This contrasts unchanged *Stat3* expression levels (Fig. 7F), elevated STAT3-target scores across all time points in Etv6Δ cells (Fig. 7G), and comparable leptin-induced fold-changes of STAT3-target genes between genotypes (Fig. 7H).

Together, these data indicate that although Etv6 deletion produced widespread genotype-dependent differences in basal gene expression that were already present before leptin stimulation and persisted throughout the time course, the relative transcriptional response to leptin was largely preserved, with only a limited subset of

Copyright © 2026 the author(s)

Downloaded from journals.bioscientifica.com/jme/article-pdf/doi/10.1530/JME-26-0065/526775/jme-26-0065.pdf by [CU-1058505] | Helmholtz Zentrum Muenchen user on 27 October 2026

genes showing altered leptin responsiveness. These findings suggest that ETV6 primarily establishes the basal transcriptional state upon which leptin-induced gene regulation is built, rather than controlling the magnitude or temporal pattern of the response.

Discussion

Leptin signaling operates through a multilayered regulatory network that is known to involve JAK2–STAT3 as a central transcriptional axis [44,45], with additional contributions from MAPK and PI3K–AKT pathways [46,47]. Although these components have been established, the temporal structure of leptin-evoked transcriptional regulation and the interaction kinetics among individual transcriptional regulators remain incompletely defined. Here, using a LepRb-overexpressing hypothalamic neuronal model and CRISPR-Cas9–engineered deletion lines, we provide a system-level analysis that resolves how leptin responses unfold over time and how distinct regulatory layers, dynamic and baseline, cooperate to shape leptin-responsive gene expression.

Using time-resolved transcriptomics, we revealed that leptin induces a structured, temporally ordered transcriptional program consisting of early (30 min) inflammatory and stress-associated genes followed by sustained cytokine- and interferon-linked transcription (180 min). These findings are consistent with the immunomodulatory functions of leptin and suggest that prolonged leptin signalling engages transcriptional programs associated with inflammatory and cytokine signalling in addition to its well-established metabolic functions. While proteomic changes were directionally aligned with these transcriptional changes, we observed a lower magnitude of protein-level alterations, which likely reflects a combination of reduced detection sensitivity in our

Copyright © 2026 the author(s)

Accepted Manuscript published as JME-26-0065. Accepted for publication: 20-Oct-2026

Downloaded from journals.bioscientifica.com/jme/article-pdf/doi/10.1530/JME-26-0065/526775/jme-26-0065.pdf by [CU-1058505] | Helmholtz Zentrum Muenchen user on 27 October 2026

assays and intrinsic biological delays due to protein turnover, translational control, or post-translational modification. More chronic exposure times, such as the 24 hours used by Octon et al. in their leptin exposure studies in CLU177 cells, may lead to better alignment between transcriptome and proteome changes, and help unmask later signaling and feedback events not covered by our experimental paradigm [48]. Overall, nonetheless, in our hands the transcriptome therefore provided a clear and robust window into the kinetics of leptin-evoked signaling and regulatory propagation.

Unsupervised clustering of leptin-responsive genes resolved three dominant temporal trajectories, EarlyUp, UpThenDown and LateUp. Regulon-based transcription factor (TF) activity inference further identified four temporally ordered TF activity modules (EarlyUp, UpThenDown, LateUp and LateDown) that aligned closely with these gene clusters, indicating coordinated regulatory states. Transient early transcriptional responses [49,50] were dominated by STAT1/3/5A, NF-κB components, and AP-1 regulators, indicating the rapid recruitment of immediate-early inflammatory and stress pathways downstream of LepRb [23,51–53]. The late-rising module, enriched for PPARG and NRF2/NFE2L2 [54–56] as well as MYC and CREB-family factors, suggested a transition toward metabolic, redox, and homeostatic remodeling programs [57–59]. Meanwhile, MEF2-associated regulons were suppressed in the late phase, indicating a shift away from steady-state neuronal maintenance [60,61]. Together, these findings outline a temporally stratified architecture of leptin signaling, in which receptor-proximal TF engagement transitions into broader cytokine- and stress-adaptation programs.

A conceptual advance of this study is the direct comparison of STAT3 and ETV6 within the same experimental framework. While STAT3's role as the principal mediator of leptin-dependent transcription and metabolic control is well established [3,4], its dynamic

Copyright © 2026 the author(s)

Downloaded from journals.bioscientifica.com/jme/article-pdf/doi/10.1530/JME-26-0065/526775/jme-26-0065.pdf by [CU-1058505] | Helmholtz Zentrum Muenchen user on 27 October 2026

contribution and hierarchical interactions with downstream repressors have been less clear. Here, *Stat3* deletion profoundly altered basal transcription and disrupted both early and late leptin-induced responses. The STAT3 target signature and JAK–STAT pathway scores were diminished at baseline, and leptin induction of both EarlyUp and LateUp modules was markedly blunted. Many late-phase transcripts even exhibited genotype-dependent reversals in directionality. These findings confirm STAT3 as the key regulator for initiating leptin-induced transcription that also governs a later and sustained cytokine-associated transcriptional phase.

Importantly, we observed increased STAT1, CREB1, and MAPK activities in Stat3Δ cells, revealing adaptive network rewiring in the absence of a key signaling hub. These changes are consistent with prior observations that loss of STAT3 in LepRb neurons of mice induces STAT1 expression, although STAT1 alone cannot rescue energy-balance defects [62]. Our temporal data expands on these observations by showing that alternative pathways are engaged progressively during the late phase yet remain insufficient to restore canonical leptin-induced dynamics. Thus, STAT3 functions as central architect of leptin-evoked transcriptional responses, and its loss reveals the plasticity, but also the limits, of adaptive signaling.

In contrast, deletion of ETV6, a STAT3-regulated transcriptional repressor recently found to be increased by leptin exposure in *LepRb*-positive neurons [28–31], uncovered a distinct regulatory function. Etv6Δ cells exhibited extensive baseline transcriptional rewiring, particularly increased expression of STAT3 target genes, confirming ETV6's role as a downstream repressor. Strikingly, however, leptin-induced transcriptional dynamics were largely preserved. Only a small set of *Etv6*-specific leptin-responsive genes was identified, including *Nox4*, associated with H_2O_2-mediated enhancement of JAK2 and

Copyright © 2026 the author(s)

 Accepted Manuscript published as JME-26-0065. Accepted for publication: 20-Oct-2026

Downloaded from journals.bioscientifica.com/jme/article-pdf/doi/10.1530/JME-26-0065/526775/jme-26-0065.pdf by [CU-1058505] | Helmholtz Zentrum Muenchen user on 27 October 2026

STAT3 phosphorylation [63], and *Peg10*, a retrotransposon-derived transcriptional regulator [64]. However, although both genes showed reduced inducibility in Etv6Δ cells, their functional contributions to the altered transcriptional response remain to be investigated. Moreover, leptin-induced fold changes of *Nox4* and *Peg10* were comparable to WT. These findings demonstrate that ETV6 primarily shapes the steady-state transcriptional landscape via gene repression. Although leptin induces Etv6 expression, suggesting a potential negative feedback mechanism, deletion of Etv6 elevated STAT3 target gene expression similarly at baseline and after leptin stimulation. The magnitude of the leptin-induced response thus remained preserved. Within the acute time frame examined here, ETV6 function appears to solely influence the basal transcriptional set point rather than substantially modulating dynamic leptin-induced transcriptional responses.

This contrasting regulatory role observed in Stat3Δ and Etv6Δ cells illustrates two mechanistically distinct modes of transcriptional control in leptin signaling. First, a dynamic module shaped by STAT3 that governs immediate and sustained leptin responses indispensable for the control of metabolic homeostasis [44,62]. Second, a baseline module - shaped by ETV6 - that tunes the transcriptional baseline without affecting the responsiveness to leptin. This conceptual distinction may further help interpreting why non-STAT3 signaling regulons and pathways, although engaged and contributing to late-phase network rewiring, may exert only limited physiological impact on energy homeostasis in mice. Mouse genetic studies show negligible metabolic effects after *Stat1* and *Stat5* deletion from *LepRb*-expressing neurons, whereas STAT3 alone is sufficient to drive leptin-induced effects on energy balance [62], highlighting that STAT3 is the only STAT with clear metabolic relevance in vivo. However, these conclusions arise

Copyright © 2026 the author(s)

Downloaded from journals.bioscientifica.com/jme/article-pdf/doi/10.1530/JME-26-0065/526775/jme-26-0065.pdf by [CU-1058505] | Helmholtz Zentrum Muenchen user on 27 October 2026

from global LepR^{Cre}-driven deletions across all *LepRb*-expressing cell populations, even though *LepR* is distributed unevenly among neuronal and non-neuronal cell types in the mouse brain. Along that line, STAT3 was shown to be dispensable for leptin actions on reproduction, and LepR^{Cre}-specific *Stat3* knockouts display milder phenotypes compared to Lep^{ob} or Lep^{db} mice [4,44,65]. Differences in *LepR* abundance, the leptin signaling architecture or cellular context therefore remain unresolved by these models, and our hypothalamic cell system equally cannot capture this heterogeneity. Moreover, transcriptomic data alone are insufficient to fully replace information on leptin-induced changes in membrane excitability and other electrophysiological responses, which represent critical determinants of neuronal function. Accordingly, the apparent lack of contribution from non-STAT3 pathways may be partially masked by these experimental limitations.

In summary, our findings define a temporally layered architecture of leptin signaling in hypothalamic neurons, in which early STAT□, NF□κB□, and AP□1–driven transcription transitions into sustained cytokine□associated programs. STAT3 emerges as a central regulator of both phases, whereas ETV6 primarily modulates the baseline transcriptional tone. These results refine our understanding of leptin□responsive regulatory networks and highlight the importance of combining temporal resolution with genetic dissection to uncover compensatory and hierarchical interactions. Future work integrating in vivo systems, finer temporal sampling with intermediate and later time points, and post□transcriptional measurements will be essential to fully reconstruct the multilayered signaling architecture through which leptin regulates neuronal function and energy balance.

Copyright © 2026 the author(s)

 Accepted Manuscript published as JME-26-0065. Accepted for publication: 20-Oct-2026

Downloaded from journals.bioscientifica.com/jme/article-pdf/doi/10.1530/JME-26-0065/526775/jme-26-0065.pdf by [CU-1058505] | Helmholtz Zentrum Muenchen user on 27 October 2026

References

1. Rosenbaum M, Leibel RL. Role of leptin in energy homeostasis in humans. *J Endocrinol*. 2014;223(1):T83-T96. doi:10.1530/JOE-14-0358
2. Friedman J. 20 YEARS OF LEPTIN: Leptin at 20: an overview. *Journal of Endocrinology*. 2014;223(1):T1-T8. doi:10.1530/JOE-14-0405
3. Banks AS, Davis SM, Bates SH, Myers MG. Activation of Downstream Signals by the Long Form of the Leptin Receptor*. *Journal of Biological Chemistry*. 2000;275(19):14563-14572. doi:10.1074/jbc.275.19.14563
4. Bates SH, Stearns WH, Dundon TA, et al. STAT3 signalling is required for leptin regulation of energy balance but not reproduction. *Nature*. 2003;421(6925):856-859. doi:10.1038/nature01388
5. Cui Y, Huang L, Elefteriou F, et al. Essential Role of STAT3 in Body Weight and Glucose Homeostasis. *Molecular and Cellular Biology*. 2004;24(1):258-269. doi:10.1128/MCB.24.1.258-269.2004
6. Gao Q, Wolfgang MJ, Neschen S, et al. Disruption of neural signal transducer and activator of transcription 3 causes obesity, diabetes, infertility, and thermal dysregulation. *Proc Natl Acad Sci U S A*. 2004;101(13):4661-4666. doi:10.1073/pnas.0303992101
7. Frühbeck G, Gómez-Ambrosi J, Martínez JA. Pre- and postprandial expression of the leptin receptor splice variants OB-Ra and OB-Rb in murine peripheral tissues. *Physiol Res*. 1999;48(3):189-195.
8. Pardo M, Roca-Rivada A, Al-Massadi O, Seoane LM, Camiña JP, Casanueva FF. Peripheral leptin and ghrelin receptors are regulated in a tissue-specific manner in activity-based anorexia. *Peptides*. 2010;31(10):1912-1919. doi:10.1016/j.peptides.2010.06.022
9. Elmquist JK, Maratos-Flier E, Saper CB, Flier JS. Unraveling the central nervous system pathways underlying responses to leptin. *Nat Neurosci*. 1998;1(6):445-450. doi:10.1038/2164
10. Fei H, Okano HJ, Li C, et al. Anatomic localization of alternatively spliced leptin receptors (Ob-R) in mouse brain and other tissues. *Proceedings of the National Academy of Sciences*. 1997;94(13):7001-7005. doi:10.1073/pnas.94.13.7001
11. Robertson SA, Leinninger GM, Myers MG. Molecular and neural mediators of leptin action. *Physiol Behav*. 2008;94(5):637-642. doi:10.1016/j.physbeh.2008.04.005
12. Krashes MJ, Koda S, Ye C, et al. Rapid, reversible activation of AgRP neurons drives feeding behavior in mice. *J Clin Invest*. 2011;121(4):1424-1428. doi:10.1172/JCI46229
13. Xu J, Bartolome CL, Low CS, et al. Genetic identification of leptin neural circuits in energy and glucose homeostases. *Nature*. 2018;556(7702):505-509. doi:10.1038/s41586-018-0049-7
14. Campbell JN, Macosko EZ, Fenselau H, et al. A molecular census of arcuate hypothalamus and median eminence cell types. *Nat Neurosci*. 2017;20(3):484-496. doi:10.1038/nn.4495

Copyright © 2026 the author(s)

15. Baumann H, Morella KK, White DW, et al. The full-length leptin receptor has signaling capabilities of interleukin 6-type cytokine receptors. *Proc Natl Acad Sci U S A*. 1996;93(16):8374-8378. doi:10.1073/pnas.93.16.8374
16. Pérez-Pérez A, Gambino Y, Maymó J, et al. MAPK and PI3K activities are required for leptin stimulation of protein synthesis in human trophoblastic cells. *Biochem Biophys Res Commun*. 2010;396(4):956-960. doi:10.1016/j.bbrc.2010.05.031
17. Saxena NK, Sharma D, Ding X, et al. Concomitant activation of the JAK/STAT, PI3K/AKT, and ERK signaling is involved in leptin-mediated promotion of invasion and migration of hepatocellular carcinoma cells. *Cancer Res*. 2007;67(6):2497-2507. doi:10.1158/0008-5472.CAN-06-3075
18. Jayavelu AK, Liu JJ, Schriever SC, et al. EasyAb: A High-Throughput Workflow for Antibody-Based PTM Peptide Enrichment Method Coupled to Mass Spectrometry. *bioRxiv*. Preprint posted online November 1, 2024:2024.10.29.620939. doi:10.1101/2024.10.29.620939
19. Beutler LR, Chen Y, Ahn JS, Lin YC, Essner RA, Knight ZA. Dynamics of Gut-Brain Communication Underlying Hunger. *Neuron*. 2017;96(2):461-475.e5. doi:10.1016/j.neuron.2017.09.043
20. Bence KK, Delibegovic M, Xue B, et al. Neuronal PTP1B regulates body weight, adiposity and leptin action. *Nat Med*. 2006;12(8):917-924. doi:10.1038/nm1435
21. Bjørbæk C, El-Haschimi K, Frantz JD, Flier JS. The Role of SOCS-3 in Leptin Signaling and Leptin Resistance*. *Journal of Biological Chemistry*. 1999;274(42):30059-30065. doi:10.1074/jbc.274.42.30059
22. Lee JY, Muenzberg H, Gavrilova O, et al. Loss of Cytokine-STAT5 Signaling in the CNS and Pituitary Gland Alters Energy Balance and Leads to Obesity. *PLOS ONE*. 2008;3(2):e1639. doi:10.1371/journal.pone.0001639
23. Kwon O, Kim KW, Kim MS. Leptin signalling pathways in hypothalamic neurons. *Cell Mol Life Sci*. 2016;73(7):1457-1477. doi:10.1007/s00018-016-2133-1
24. Zhang X, Zhang G, Zhang H, Karin M, Bai H, Cai D. Hypothalamic IKKbeta/NF-kappaB and ER stress link overnutrition to energy imbalance and obesity. *Cell*. 2008;135(1):61-73. doi:10.1016/j.cell.2008.07.043
25. Gahlot S, Caron A, Lee S, Elmquist JK. THU128 Transcription Factor ETV5 In POMC Neurons Regulate Energy And Glucose Homeostasis. *J Endocr Soc*. 2023;7(Suppl 1):bvad114.002. doi:10.1210/jendso/bvad114.002
26. Gutierrez-Aguilar R, Kim DH, Casimir M, et al. The role of the transcription factor ETV5 in insulin exocytosis. *Diabetologia*. 2014;57(2):383-391. doi:10.1007/s00125-013-3096-5
27. Schick N, Oakeley EJ, Hynes NE, Badache A. TEL/ETV6 is a signal transducer and activator of transcription 3 (Stat3)-induced repressor of Stat3 activity. *J Biol Chem*. 2004;279(37):38787-38796. doi:10.1074/jbc.M312581200
28. Belmont-Rausch DM, Kapel BS, Tomlinson AJ, et al. A uniquely leptin sensitive hypothalamic neuron population limits hyperphagia and weight gain in diet-induced obesity. *bioRxiv*. Preprint posted online March 30, 2026:2026.03.26.714161. doi:10.64898/2026.03.26.714161
29. Heyward FD, Liu N, Jacobs C, et al. AgRP neuron cis-regulatory analysis across hunger states reveals that IRF3 mediates leptin's acute effects. *Nat Commun*. 2024;15:4646. doi:10.1038/s41467-024-48885-y

Downloaded from journals.bioscientifica.com/jme/article-pdf/doi/10.1530/JME-26-0065/526775/jme-26-0065.pdf by [CU-1058505] | Helmholtz Zentrum Muenchen user on 27 October 2026

Copyright © 2026 the author(s)

Accepted Manuscript published as JME-26-0065. Accepted for publication: 20-Oct-2026

Downloaded from journals.bioscientifica.com/jme/article-pdf/doi/10.1530/JME-26-0065/526775/jme-26-0065.pdf by [CU-1058505] | Helmholtz Zentrum Muenchen user on 27 October 2026

30. Inoue F, Eckalbar WL, Wang Y, et al. Genomic and epigenomic mapping of leptin-responsive neuronal populations involved in body weight regulation. *Nat Metab*. 2019;1(4):475-484. doi:10.1038/s42255-019-0051-x
31. Allison MB, Pan W, MacKenzie A, et al. Defining the Transcriptional Targets of Leptin Reveals a Role for Atf3 in Leptin Action. *Diabetes*. 2018;67(6):1093-1104. doi:10.2337/db17-1395
32. Grosche A, Hauser A, Lepper MF, et al. The Proteome of Native Adult Müller Glial Cells From Murine Retina. *Mol Cell Proteomics*. 2016;15(2):462-480. doi:10.1074/mcp.M115.052183
33. Wiśniewski JR, Zougman A, Nagaraj N, Mann M. Universal sample preparation method for proteome analysis. *Nat Methods*. 2009;6(5):359-362. doi:10.1038/nmeth.1322
34. Cong L, Ran FA, Cox D, et al. Multiplex genome engineering using CRISPR/Cas systems. *Science*. 2013;339(6121):819-823. doi:10.1126/science.1231143
35. Steuernagel L, Lam BYH, Klemm P, et al. HypoMap—a unified single-cell gene expression atlas of the murine hypothalamus. *Nat Metab*. 2022;4(10):1402-1419. doi:10.1038/s42255-022-00657-y
36. Tian B, Nowak DE, Brasier AR. A TNF-induced gene expression program under oscillatory NF-κB control. *BMC Genomics*. 2005;6:137. doi:10.1186/1471-2164-6-137
37. Zambrano S, Loffreda A, Carelli E, et al. First Responders Shape a Prompt and Sharp NF-κB-Mediated Transcriptional Response to TNF-α. *iScience*. 2020;23(9). doi:10.1016/j.isci.2020.101529
38. Abbasi Kasbi N, Stopschinski BE, Polyak AG, et al. Leptin as a Potential Modifier of Neuroinflammation: Contrasting Roles in Alzheimer's Disease and Multiple Sclerosis. *Int J Mol Sci*. 2025;27(1):168. doi:10.3390/ijms27010168
39. Garcia-Alonso L, Holland CH, Ibrahim MM, Turei D, Saez-Rodriguez J. Benchmark and integration of resources for the estimation of human transcription factor activities. *Genome Res*. 2019;29(8):1363-1375. doi:10.1101/gr.240663.118
40. Schubert M, Klinger B, Klünemann M, et al. Perturbation-response genes reveal signaling footprints in cancer gene expression. *Nat Commun*. 2018;9(1):20. doi:10.1038/s41467-017-02391-6
41. Wang Z, Mehra V, Simpson MT, et al. KLF6 and STAT3 co-occupy regulatory DNA and functionally synergize to promote axon growth in CNS neurons. *Sci Rep*. 2018;8(1):12565. doi:10.1038/s41598-018-31101-5
42. Hock H, Meade E, Medeiros S, et al. Tel/Etv6 is an essential and selective regulator of adult hematopoietic stem cell survival. *Genes Dev*. 2004;18(19):2336-2341. doi:10.1101/gad.1239604
43. Neveu B, Richer C, Cassart P, et al. Identification of new ETV6 modulators through a high-throughput functional screening. *iScience*. 2022;25(3):103858. doi:10.1016/j.isci.2022.103858
44. Piper ML, Unger EK, Myers MG Jr, Xu AW. Specific Physiological Roles for Signal Transducer and Activator of Transcription 3 in Leptin Receptor-Expressing Neurons. *Mol Endocrinol*. 2008;22(3):751-759. doi:10.1210/me.2007-0389
45. Vaisse C, Halaas JL, Horvath CM, Darnell JE, Stoffel M, Friedman JM. Leptin activation of Stat3 in the hypothalamus of wild–type and ob/ob mice but not db/db mice. *Nat Genet*. 1996;14(1):95-97. doi:10.1038/ng0996-95

Copyright © 2026 the author(s)

46. Bjørbaek C, Uotani S, da Silva B, Flier JS. Divergent signaling capacities of the long and short isoforms of the leptin receptor. *J Biol Chem*. 1997;272(51):32686-32695. doi:10.1074/jbc.272.51.32686
47. Saxena NK, Titus MA, Ding X, et al. Leptin as a novel profibrogenic cytokine in hepatic stellate cells: mitogenesis and inhibition of apoptosis mediated by extracellular regulated kinase (Erk) and Akt phosphorylation. *FASEB J*. 2004;18(13):1612-1614. doi:10.1096/fj.04-1847fje
48. Ocłoń E, Gurgul A, Szmatoła T, et al. Impact of modulating leptin sensitivity on the transcriptomic profile of adult-derived hypothalamic mouse neurons. *Front Mol Neurosci*. 2025;17. doi:10.3389/fnmol.2024.1518737
49. Bjørbaek C, Buchholz RM, Davis SM, et al. Divergent roles of SHP-2 in ERK activation by leptin receptors. *J Biol Chem*. 2001;276(7):4747-4755. doi:10.1074/jbc.M007439200
50. Pagel JI, Deindl E. Early growth response 1--a transcription factor in the crossfire of signal transduction cascades. *Indian J Biochem Biophys*. 2011;48(4):226-235.
51. Bendinelli P, Maroni P, Pecori Giraldi F, Piccoletti R. Leptin activates Stat3, Stat1 and AP-1 in mouse adipose tissue. *Mol Cell Endocrinol*. 2000;168(1-2):11-20. doi:10.1016/s0303-7207(00)00313-0
52. Park HK, Ahima RS. Leptin signaling. *F1000Prime Rep*. 2014;6:73. doi:10.12703/P6-73
53. Procaccini C, Lourenco EV, Matarese G, La Cava A. Leptin signaling: A key pathway in immune responses. *Curr Signal Transduct Ther*. 2009;4(1):22-30. doi:10.2174/157436209787048711
54. Daniel Y, Rauch C, Moutaux L, et al. PPARγ, a key modulator of metabolic reprogramming, stemness and chemoresistance associated with retrodifferentiation in human hepatocellular carcinomas. *Cell Death Dis*. 2025;16(1):831. doi:10.1038/s41419-025-07799-3
55. Xue P, Hou Y, Chen Y, et al. Adipose deficiency of Nrf2 in ob/ob mice results in severe metabolic syndrome. *Diabetes*. 2013;62(3):845-854. doi:10.2337/db12-0584
56. Yagishita Y, Uruno A, Fukutomi T, et al. Nrf2 Improves Leptin and Insulin Resistance Provoked by Hypothalamic Oxidative Stress. *Cell Rep*. 2017;18(8):2030-2044. doi:10.1016/j.celrep.2017.01.064
57. Gutiérrez-Tenorio J, Marín-Royo G, Martínez-Martínez E, et al. The role of oxidative stress in the crosstalk between leptin and mineralocorticoid receptor in the cardiac fibrosis associated with obesity. *Sci Rep*. 2017;7(1):16802. doi:10.1038/s41598-017-17103-9
58. Hosoi T, Sasaki M, Miyahara T, et al. Endoplasmic reticulum stress induces leptin resistance. *Mol Pharmacol*. 2008;74(6):1610-1619. doi:10.1124/mol.108.050070
59. Smith BS, Diaguarachchige De Silva KH, Hashemi A, et al. Transcription factor CREB3 is a potent regulator of high-fat diet-induced obesity and energy metabolism. *Int J Obes (Lond)*. 2022;46(8):1446-1455. doi:10.1038/s41366-022-01128-w
60. Flavell SW, Cowan CW, Kim TK, et al. Activity-dependent regulation of MEF2 transcription factors suppresses excitatory synapse number. *Science*. 2006;311(5763):1008-1012. doi:10.1126/science.1122511
61. Zhu B, Carmichael RE, Solabre Valois L, Wilkinson KA, Henley JM. The transcription factor MEF2A plays a key role in the differentiation/maturation of rat neural stem

Downloaded from journals.bioscientifica.com/jme/article-pdf/doi/10.1530/JME-26-0065/526775/jme-26-0065.pdf by [CU-1058505] | Helmholtz Zentrum Muenchen user on 27 October 2026

Copyright © 2026 the author(s)

 Accepted Manuscript published as JME-26-0065. Accepted for publication: 20-Oct-2026

cells into neurons. *Biochem Biophys Res Commun*. 2018;500(3):645-649. doi:10.1016/j.bbrc.2018.04.125
62. Pan W, Allison MB, Sabatini P, et al. Transcriptional and physiological roles for STAT proteins in leptin action. *Mol Metab*. 2019;22:121-131. doi:10.1016/j.molmet.2019.01.007
63. Fruhwürth S, Vogel H, Schürmann A, Williams KJ. Novel Insights into How Overnutrition Disrupts the Hypothalamic Actions of Leptin. *Front Endocrinol*. 2018;9. doi:10.3389/fendo.2018.00089
64. Steplewski A, Krynska B, Tretiakova A, Haas S, Khalili K, Amini S. MyEF-3, a developmentally controlled brain-derived nuclear protein which specifically interacts with myelin basic protein proximal regulatory sequences. *Biochem Biophys Res Commun*. 1998;243(1):295-301. doi:10.1006/bbrc.1997.7821
65. Jiang L, You J, Yu X, et al. Tyrosine-dependent and -independent actions of leptin receptor in control of energy balance and glucose homeostasis. *Proc Natl Acad Sci U S A*. 2008;105(47):18619-18624. doi:10.1073/pnas.0804589105

Acknowledgement

We thank Katrin Huber and Miriam Krekel for technical assistance. RGA wants to thank the Universidad Nacional Autónoma de México and Dirección General de Asuntos del Personal Académico (UNAM/DGAPA/PASPA) for the stipend given during the sabbatical year. The mObRb plasmid was a kind gift of Yves Rouillé (Université de Lille, France), the pCA & 2A-H2B plasmid was a kind gift of Ingo Burtscher (Helmholtz Munich, Germany). Schematics were created with BioRender.com. We further acknowledge the technical support of the Core Facilities Monoclonal Antibodies (CF-MAB), Genomics (CF-GEN) and Metabolomics and Proteomics (CF-MPC) at Helmholtz Munich. We thank Dr Gertrud Eckstein, Dr. Inti de la Rosa, Dr. Stefanie Hauck and Dr. Juliane Merl-Pham for their help with the library synthesis, RNA sequencing and proteomics, respectively.

Downloaded from journals.bioscientifica.com/jme/article-pdf/doi/10.1530/JME-26-0065/526775/jme-26-0065.pdf by [CU-1058505] | Helmholtz Zentrum Muenchen user on 27 October 2026

Copyright © 2026 the author(s)

Downloaded from journals.bioscientifica.com/jme/article-pdf/doi/10.1530/JME-26-0065/526775/jme-26-0065.pdf by [CU-1058505] | Helmholtz Zentrum Muenchen user on 27 October 2026

Funding

This work was funded by the European Research Council ERC-CoG Yoyo-LepReSens no. 101002247, awarded to PTP, and by the German Center for Diabetes Research (DZD). MB was supported through the International Helmholtz Research School for Diabetes, funded by the Helmholtz Association—Initiative and Networking Fund.

Author statement

EP, MB, RGA, SCS & PTP conceptualized and designed all experiments; SCS generated the cell line; MB, NM, CM, SCS conducted all cell experiments; NM, SCS prepared libraries; AK performed proteomics. EP performed bioinformatical analyses; EP, SCS and PTP wrote the manuscript. All authors revised the manuscript.

Conflict of Interest Statement

PTP received speaker honoraria from Novo Nordisk. All other authors declare that they have no conflict of interest related to this study.

Data Availability

This manuscript contains Supplemental Material published as online version. RNA-seq data have been deposited in the ArrayExpress database at EMBL-EBI (www.ebi.ac.uk/arrayexpress) under accession number E-MTAB-16711. The mass

Copyright © 2026 the author(s)

 Accepted Manuscript published as JME-26-0065. Accepted for publication: 20-Oct-2026

spectrometry proteomics data have been deposited to the ProteomeXchange Consortium via the PRIDE repository at EMBL-EBI (www.ebi.ac.uk/pride) with the dataset identifier PXD076275. Custom R code used for sequencing and proteome data analysis and visualization has been deposited in a public GitHub repository maintained by E. Pathak and is available at https://github.com/ektapathak08. Further material is available from the corresponding author upon reasonable request.

Downloaded from journals.bioscientifica.com/jme/article-pdf/doi/10.1530/JME-26-0065/526775/jme-26-0065.pdf by [CU-1058505] | Helmholtz Zentrum Muenchen user on 27 October 2026

Copyright © 2026 the author(s)

Downloaded from journals.bioscientifica.com/jme/article-pdf/doi/10.1530/JME-26-0065/526775/jme-26-0065.pdf by [CU-1058505] | Helmholtz Zentrum Muenchen user on 27 October 2026

Figures legends

Fig. 1. Generation and validation of a leptin receptor-expressing hypothalamic cell line.

(**A**) Schematic for the generation of CLU177mOBRb cells stably expressing the long leptin receptor isoform and their subsequent leptin-stimulation for Western Blotting (WB) and immunofluorescence (IF) microscopy. (**B**) Representative WB of CLU177mOBRb cells treated with increasing doses of leptin for 20 min. (**C**) Densitometric analysis of WBs for phospho (P)-STAT3 vs. β-ACTIN (n=3-4). (**D**) IF microscopy confirmed the induction of P-STAT3 after 20 min and 10 nM of leptin exposure, compared to untreated controls. (**E**) *Atf3*, *Socs3*, and *Steap4* mRNA levels following leptin exposure for 30, 60, 180 and 300 min, determined by quantitative PCR (n=9-11). (**F**) Schematic for transcriptome and proteome measurements in CLU177mOBRb cells following 0, 30 and 180 min of leptin exposure. (**G**) PCA of WT transcriptomes (0, 30, 180 min), showing separation by leptin exposure time (n=8). (**H**) PCA of WT proteomes (0 and 180 min), showing time-dependent separation (n=3-4). (**I**) Numbers of significantly up- and down-regulated DEGs/DAPs at 30 and 180 min. (**J**) Scatter plot showing the Spearman correlation of signed significance ($-\log_{10} P \times$ sign fold change (FC)) between transcriptomic and proteomic changes at 180 min vs 0 min leptin treatment. Means ± SEM, *p<0.05, **p<0.01, ***p<0.001, ****p<0.0001.

Fig. 2. Leptin-induced transcriptional dynamics in CLU177mOBRb (WT) cells.

(**A**) Schematic for CLU177mOBRb (WT) cells undergoing leptin exposure for RNA-sequencing. (**B**) Volcano plots showing differentially expressed genes (DEGs) in WT cells

Copyright © 2026 the author(s)

 Accepted Manuscript published as JME-26-0065. Accepted for publication: 20-Oct-2026

Downloaded from journals.bioscientifica.com/jme/article-pdf/doi/10.1530/JME-26-0065/526775/jme-26-0065.pdf by [CU-1058505] | Helmholtz Zentrum Muenchen user on 27 October 2026

after 30 and 180min of leptin exposure. Points are colored according to significance and the direction of change (Benjamini-Hochberg FDR < 0.05; |log2FC| ≥ 1). (**C**) Heatmap of variance-stabilized, batch-corrected expression values for all WT time-course DEGs (n = 990), split by stimulation time (0, 30, 180 min). Genes are clustered using k-means clustering (k=5). (**D**) Cluster-mean expression trajectories showing the temporal response patterns of each cluster of genes in (**C**): Cl. 3 (EarlyUp), Cl. 4 (LateUp), Cl. 2 (UpThenDown), Cl. 1 (LateDown), and Cl. 5 (Mixed/Other). (**E**) Hallmark pathway enrichment across clusters. Dot color indicates adjusted p-value and dot size indicates the number of overlapping genes. (**F**) Comparison of leptin-responsive genes (LRGs) identified in CLU177mOBRb cells and AgRP neurons of mice. LRGs identified by Heyward et al. were projected onto the CLU177 WT leptin time course and displayed as heatmaps showing scaled expression values after K-means clustering, with distinct temporal expression profiles termed LateUp, EarlyUp/UpThenDown and LateDown. A fourth profile without consistent regulation is displayed in Suppl. Fig. 2. N=8 samples per group.

Fig. 3. Inference and dynamics of transcription factor activities during leptin exposure in WT cells.

(**A**) Workflow for inferring TF and pathway activities from WT time-course data. (**B**) Heatmap of inferred TF activities across WT samples (0, 30, 180 min), grouped into four TF regulon activity patterns (Regulons 1 - 4). Values represent scaled norm_wmean activity scores. TF activities are depicted for the top-ranked TF regulons inferred in WT, defined as the union of the top 50 TFs (by limma B-statistic) for the 30 vs 0 min and 180 vs 0 min contrasts. (**C-F**) TF activity trajectories for (**C**) Regulon 3 (EarlyUp), (**D**) Regulon 2 (UpThenDown), (**E**) Regulon 1 (LateUp) and (**F**) Regulon 4 (LateDown). (**G**) Spearman

Copyright © 2026 the author(s)

Downloaded from journals.bioscientifica.com/jme/article-pdf/doi/10.1530/JME-26-0065/526775/jme-26-0065.pdf by [CU-1058505] | Helmholtz Zentrum Muenchen user on 27 October 2026

correlations between WT gene-expression modules (k-means clusters from the WT time-course DEG heatmap; module scores computed as the mean of batch-corrected, gene-wise z-scored VST expression values per module) and inferred TF activities. (**H**) Expression dynamics of selected canonical STAT3 target genes following leptin stimulation for 30 and 180 min. Values represent batch-corrected, gene-wise z-scored VST expression. N=8 samples per group.

Fig. 4. *Stat3* deletion rewires basal transcription and leptin-responsive signaling. (A) Schematic for the CRISPR/Cas9-mediated deletion of *Stat3* and exposure of the WT and Stat3Δ cells to leptin for 0, 30, or 180 min, followed by transcriptomics (RNA-seq) and proteomics. (**B**) *Stat3* mRNA levels in WT and Stat3Δ cells following leptin exposure (n=4). (**C**) Volcano plot for differentially expressed genes at baseline (0 min). Points are colored by significance and direction (Benjamini-Hochberg FDR < 0.05; |log2FC| ≥ 1). (**D**) Heatmap of baseline DEGs (Stat3Δ vs WT at 0 min) showing scaled expression across samples, grouped by genotype. (**E**) Gene Ontology enrichment of baseline DEGs (Stat3Δ vs WT, 0 min), with dot size showing adjusted significance, color indicating regulation direction, and gene ratio on the x-axis. Differentially inferred (**F**) transcription factor (TF) and (**G**) pathway activities at baseline (0 min) comparing Stat3Δ vs WT. Activity score matrices were analyzed with limma using a genotype-only model at 0 min (~ type). Bars show the activity log2 fold change (Stat3Δ - WT) and color indicates -log10(FDR). (**H**) STAT3-target score comparing WT and Stat3Δ at baseline. STAT3 target genes were obtained from the DoRothEA mouse regulon resource by selecting STAT3 targets with confidence levels A and B, and positive mode of regulation (mor = 1). A STAT3 target signature score was computed per sample as the mean of gene-wise z-scored VST

Copyright © 2026 the author(s)

 Accepted Manuscript published as JME-26-0065. Accepted for publication: 20-Oct-2026

Downloaded from journals.bioscientifica.com/jme/article-pdf/doi/10.1530/JME-26-0065/526775/jme-26-0065.pdf by [CU-1058505] | Helmholtz Zentrum Muenchen user on 27 October 2026

expression values across the STAT3 targets. (**I**) PCA of transcriptomes across 0, 30, and 180 min leptin exposure, showing separation by genotype and time. (**J**) Overlap of up- (top) and down-(bottom) regulated genes across time points in Stat3Δ vs WT comparisons. (**K**) Volcano plot of DAPs, Stat3Δ vs WT at 0 min. Points represent proteins colored by significance and direction. (**L**) Spearman correlation of signed significance ($-\log_{10}$ p × sign FC) between DEGs and DAPs at baseline. N=4 samples per group.

Fig 5. Stat3 deletion induces compensatory regulatory network adaptations to leptin stimulation.

(**A**) Boxplots for WT and Stat3Δ cells showing leptin-induced log2 fold changes (time vs 0) of WT cluster 3 (EarlyUp) and WT cluster 4 (LateUp) gene sets at 30 and 180 min. (**B**) Perturbation of inferred TF activities in Stat3Δ cells during leptin stimulation (genotype×leptin interaction). Points indicate interaction activity at 30 min (blue) and 180 min (red). Text color denotes significance at 30 min, at 180 min, or at both time points. Displayed TF activities correspond to the regulons displayed in Fig. 3B and include only those TF that were significantly regulated at least once in the Stat3Δ:Leptin interaction analysis. (**C**) Perturbation of inferred pathway activities in Stat3Δ cells during leptin stimulation (genotype:leptin interaction), displayed as in (**B**). (**D-I**) TF target signature scores across the leptin time course for STAT3, STAT1, MAPK, CREB1, KLF6, NFKB1 for WT and Stat3Δ cells at 0, 30, and 180 min. **(J**) Volcano plots of Stat3Δ:Leptin response genes for 0 -> 30 min and 0->180 min changes. (**K**) Genes exhibiting reversed time effects (180 vs 0 min) in WT and Stat3Δ, shown as paired log2FC values (WT in blue; Stat3Δ in red). (**L**) Heatmap of a subset (padj < 0.05, |log2FC| ≥ 3) of Stat3Δ:Leptin interaction genes across WT and Stat3Δ. (**M**) Concordance between transcriptomic and proteomic

Copyright © 2026 the author(s)

Downloaded from journals.bioscientifica.com/jme/article-pdf/doi/10.1530/JME-26-0065/526775/jme-26-0065.pdf by [CU-1058505] | Helmholtz Zentrum Muenchen user on 27 October 2026

Stat3Δ:Leptin effects, shown as signed significance values (-log10(P) × sign(FC)) for overlapping features, with the corresponding Spearman correlation indicated. N=4 samples per group.

Fig. 6. *Etv6* deletion alters the basal transcriptional state.

(**A**) Schematic for the CRISPR/Cas9-mediated generation of Etv6Δ cells, followed by leptin exposure (0, 30, 180 min) and transcriptome profiling. (**B**) *Etv6* mRNA expression in WT and Etv6Δ cells exposed to leptin for 0, 30 and 180 min (n=5-6). (**C**) Baseline expression changes of known *Etv6Δ* target genes, plotted as log2FC at 0 min. (**D**) *Stat3* expression at 0 min in WT and Etv6Δ cells. (**E**) STAT3 target signature score at 0 min comparing WT and Etv6Δ cells. (**F**) PCA of Etv6Δ and WT transcriptomes showing the effects of genotype and leptin exposure time (0, 30, 180 min). (**G**) Volcano plot of baseline DEGs. Points represent genes colored by significance and direction. (**H**) Gene Ontology enrichment of baseline DEGs (Etv6Δ vs WT at 0 min), with dot size indicating adjusted significance, dot color indicating regulatory direction, and gene ratio on the x-axis. (**I**) Overlap of up- (top) and downregulated (bottom) genes in Etv6Δ vs WT comparisons across time (0, 30, 180 min). (**J**) Heatmap of selected (log2FC >=|1|; ranked by adjusted p-value) baseline DEGs across WT and Etv6Δ samples, displayed as scaled expression and annotated by functional categories. N=4 per group.

Fig. 7. Etv6 deletion modestly affects leptin-induced transcriptional and regulatory responses

(**A**) Leptin-induced transcriptional responses of WT “EarlyUp” and “LateUp” gene sets in WT and Etv6Δ cells, shown as boxplots of log2FC (t vs 0) at 30 and 180 min. (**B**) Perturbation of inferred TF activities (left) and pathway activities (right) in Etv6Δ cells

Copyright © 2026 the author(s)

 Accepted Manuscript published as JME-26-0065. Accepted for publication: 20-Oct-2026

during leptin stimulation (Etv6Δ:Leptin interaction). Points indicate interaction activity at 30 min (blue) and 180 min (red). None of the inferred TF or pathway activities reached significance for the Etv6Δ:Leptin interaction at either time point (FDR < 0.05). (**C**) Volcano plots of Etv6Δ-specific leptin stimulation time effects (Etv6Δ:Leptin interaction) for 0->30 min and 0->180 min changes. Points represent genes colored by direction and significance. (**D**) Heatmap of Etv6Δ:Leptin interaction DEGs across WT and Etv6Δ samples (FDR < 0.05; |log2FC| ≥ 0.5). Values are shown as scaled expression with genotype and time annotations. (**E**) Mean expression of representative Etv6Δ:Leptin interaction genes (*Nox4*, *Sfmbt2*, *Peg10*, *Fam13a*) in WT and Etv6Δ cells at 0, 30 and 180 min of leptin exposure. Bars show mean VST expression; error bars indicate ± SD across replicates. (**F**) *Stat3* expression; letters in **(E)** and **(F)** show significant difference between 0 and 30 min (a), 0 and 180 min (b), and 30 and 180 min (c) and (**G**) STAT3 target signature score across time in WT and Etv6Δ cells. (**H**) Leptin-induced changes in STAT3 target gene expression shown as log2FC (t vs 0) at 30 and 180 min for WT and Etv6Δ cells. N=4 samples per group.

Downloaded from journals.bioscientifica.com/jme/article-pdf/doi/10.1530/JME-26-0065/526775/jme-26-0065.pdf by [CU-1058505] | Helmholtz Zentrum Muenchen user on 27 October 2026

Copyright © 2026 the author(s)

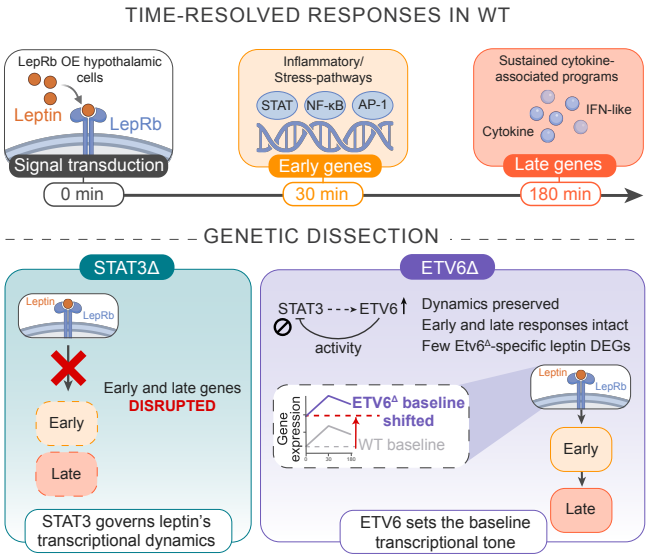

Copyright © 2026 the author(s)

Downloaded from journals.bioscientifica.com/jme/article-pdf/doi/10.1530/JME-26-0065/526775/jme-26-0065.pdf by [CU-1058505] | Helmholtz Zentrum Muenchen user on 27 October 2026

Accepted Manuscript published as JME-26-0065. Accepted for publication: 20-Oct-2026

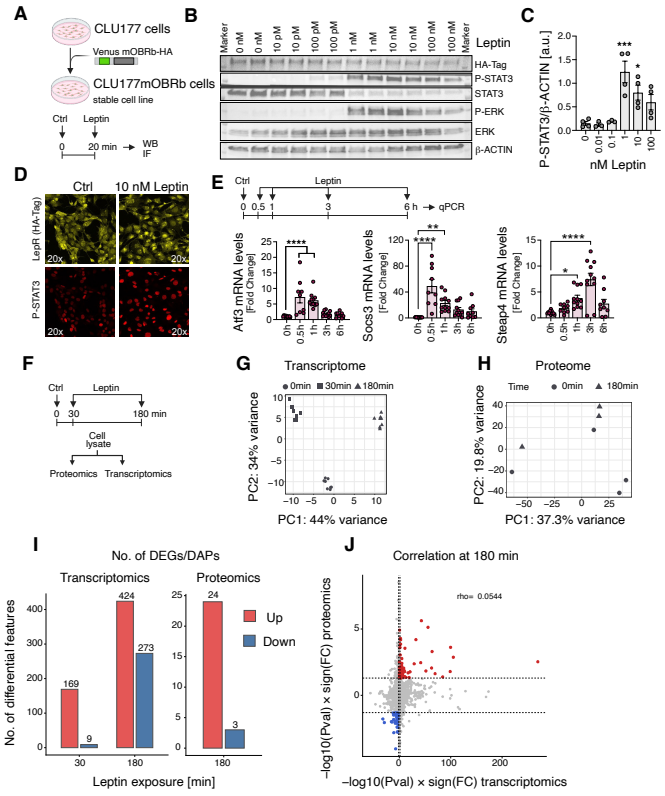

Downloaded from journals.bioscientifica.com/jme/article-pdf/doi/10.1530/JME-26-0065/526775/jme-26-0065.pdf by [CU-1058505] | Helmholtz Zentrum Muenchen user on 27 October 2026

Copyright © 2026 the author(s)

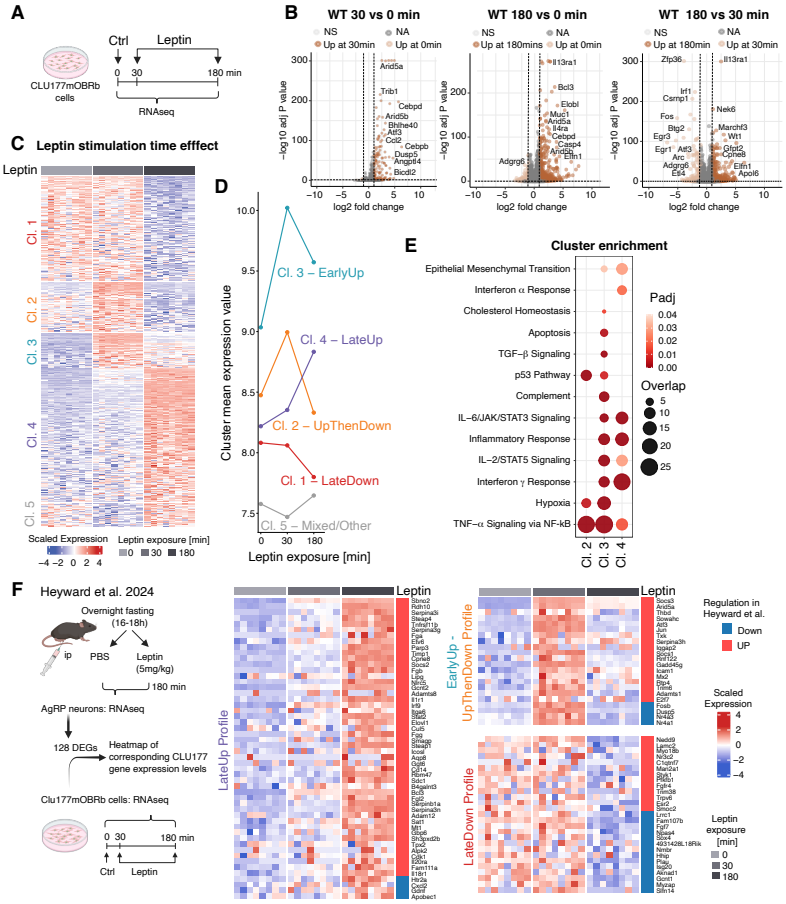

Downloaded from journals.biosciencetifica.com/jme/article-pdf/doi/10.1530/JME-26-0065/526775/jme-26-0065.pdf by [CU-1058505] | Helmholtz Zentrum Muenchen user on 27 October 2026

Copyright © 2026 the author(s)

Accepted Manuscript published as JME-26-0065. Accepted for publication: 20-Oct-2026

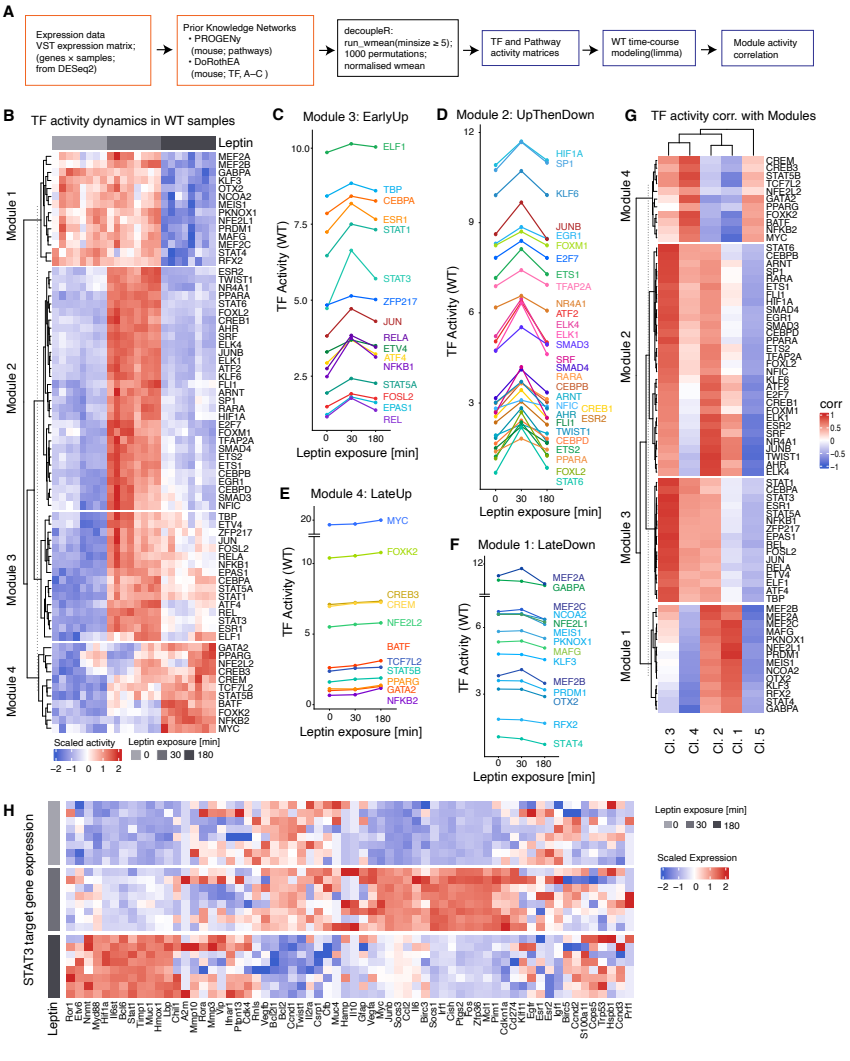

Copyright © 2026 the author(s)

Downloaded from journals.biosciencetifica.com/jme/article-pdf/doi/10.1530/JME-26-0065/526775/jme-26-0065.pdf by [CU-1058505] | Helmholtz Zentrum Muenchen user on 27 October 2026

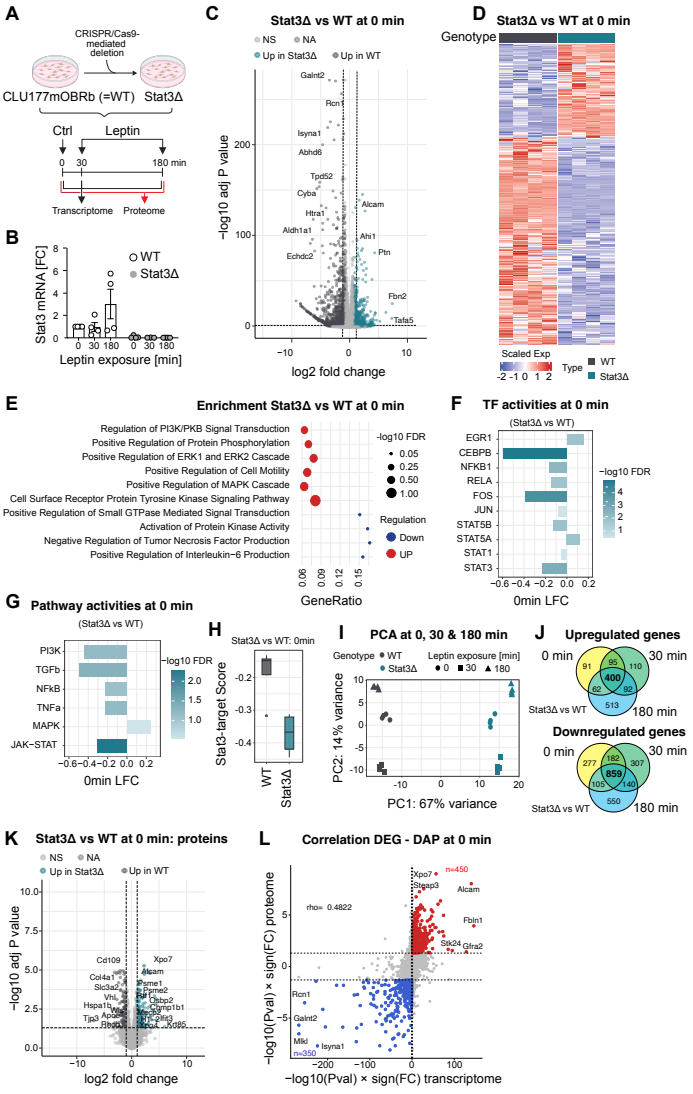

Downloaded from journals.bioscientifica.com/jme/article-pdf/doi/10.1530/JME-26-0065/526775/jme-26-0065.pdf by [CU-1058505] | Helmholtz Zentrum Muenchen user on 27 October 2026

Copyright © 2026 the author(s)

Accepted Manuscript published as JME-26-0065. Accepted for publication: 20-Oct-2026

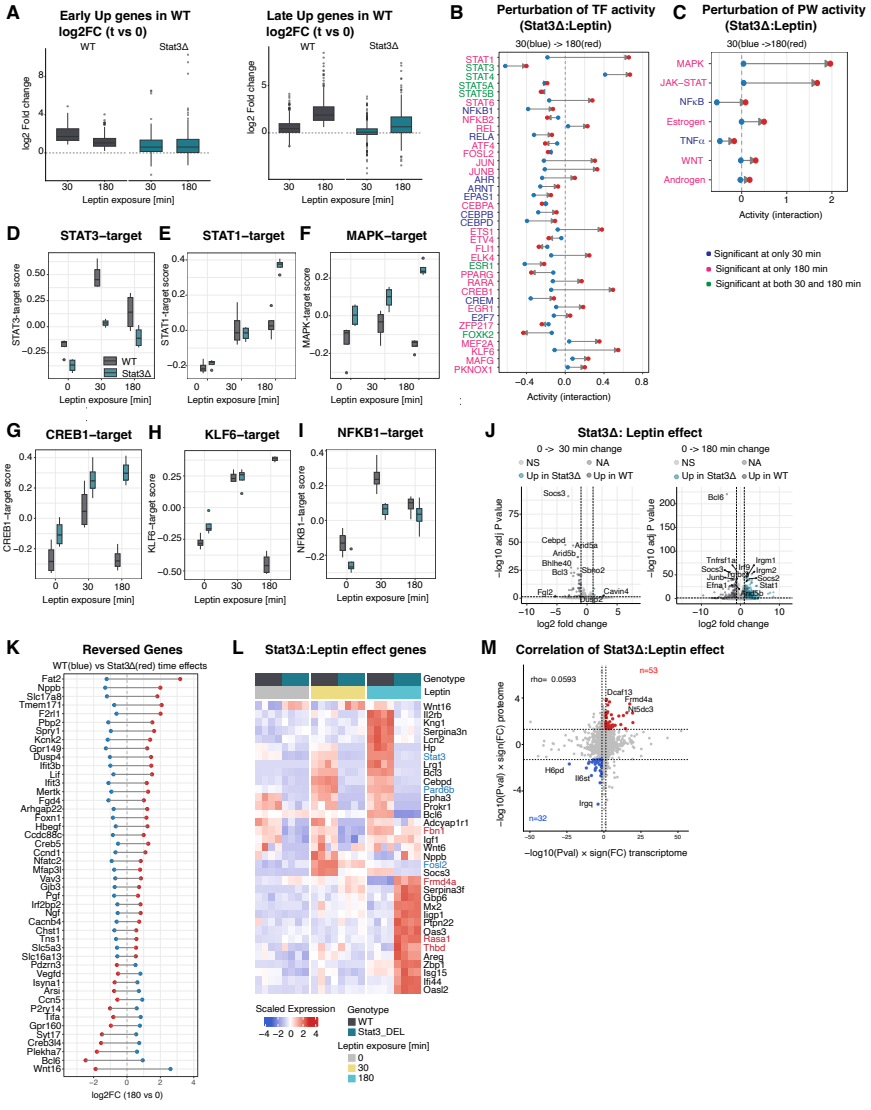

Copyright © 2026 the author(s)

Downloaded from journals.biosciencetifica.com/jme/article-pdf/doi/10.1530/JME-26-0065/526775/jme-26-0065.pdf by [CU-1058505] | Helmholtz Zentrum Muenchen user on 27 October 2026

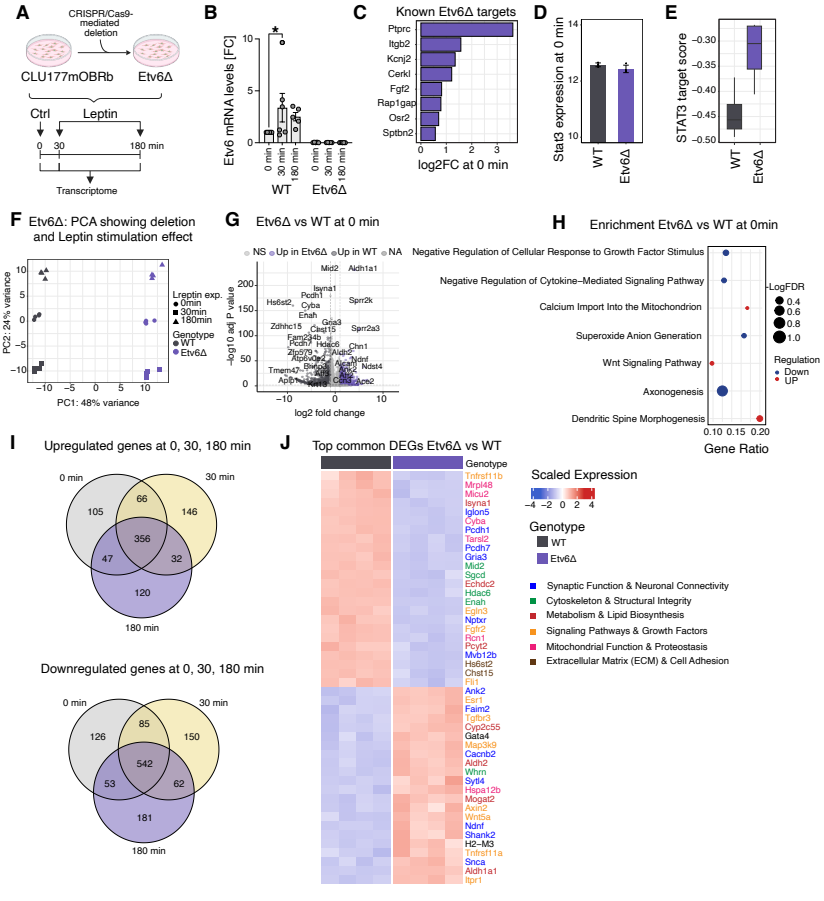

Downloaded from journals.bioscientifica.com/jme/article-pdf/doi/10.1530/JME-26-0065/526775/jme-26-0065.pdf by [CU-1058505] | Helmholtz Zentrum Muenchen user on 27 October 2026

Copyright © 2026 the author(s)

Accepted Manuscript published as JME-26-0065. Accepted for publication: 20-Oct-2026

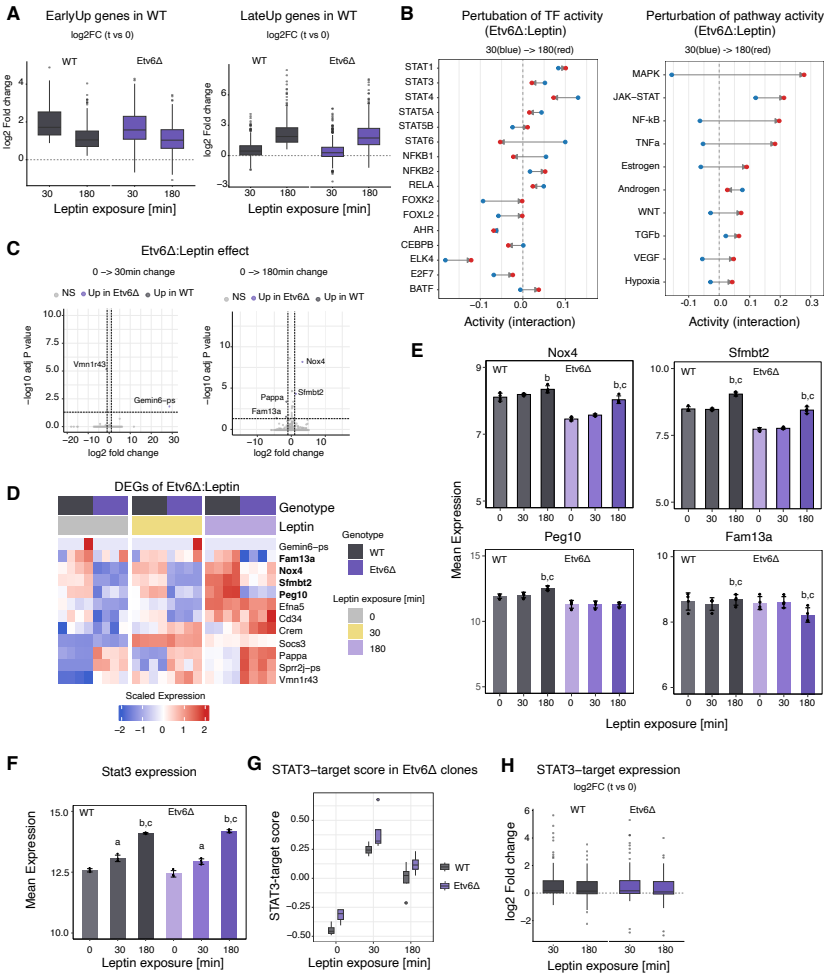

Copyright © 2026 the author(s)

Downloaded from journals.bioscientifica.com/jme/article-pdf/doi/10.1530/JME-26-0065/526775/jme-26-0065.pdf by [CU-1058505] | Helmholtz Zentrum Muenchen user on 27 October 2026